Journal of Applied Electrochemistry **31**: 863–870, 2001.

Vapour–liquid slip in a parallel-plate electrochemical fluorination reactor

K. JHA[1], G.L. BAUER[2] and J.W. WEIDNER[1,*]
[1]*Center for Electrochemical Engineering, Department of Chemical Engineering, University of South Carolina, Columbia SC 29208, USA*
[2]*3M Chemicals, St. Paul MN 55144-1000, USA*
*(*author for correspondence)*

Received 13 September 1999; accepted in revised form 28 March 2000

Key words: fluorination reactor, vapour–liquid slip

Abstract

A mathematical model was used to study the effect of slip between the gas and liquid phases on the performance of an electrochemical fluorination reactor. The model incorporates two-phase flow with differential material, energy and pressure balances. The effect of slip on the temperature, pressure, gas fraction and current distribution in the reactor is presented under relatively severe operating conditions. In addition, the effect of slip on the cell voltage, current efficiency and energy usage is shown at different flow rates over a wide current range. It was found that slip of the gas past the liquid is insignificant under normal operating conditions, but it is significant at high cell currents and low flow rates. Under these more severe operating conditions, slip significantly reduces the cell voltage, and hence the energy usage, since less gas resides in the reactor.

List of symbols

d	separation gap between the plates in the cell pack (cm)
f'	frictional factor multiplier
g	gravitational acceleration (981 cm s^{-2} or 9.81 m s^{-2})
L	length of each electrode in the cell pack (cm)
n	number of electrode pairs in the cell pack
$\dot{N}$	superficial molar flux of the two-phase mixture (mol cm^{-2} s^{-1})
$\dot{N}_l$	superficial molar flux of the liquid phase (mol cm^{-2} s^{-1})
$\dot{N}_v$	superficial molar flux of the vapour phase (mol cm^{-2} s^{-1})
P	total pressure (Pa)
T	temperature (K)
v	two-phase mixture velocity (cm s^{-1})
v_v	superficial vapour velocity (cm s^{-1})
$v_{v,drift}$	drift velocity of the vapour (cm s^{-1})
w	width of each electrode in the cell pack (cm)
x_l	molar flux of liquid per molar flux of the two-phase mixture ($\dot{N}_l/\dot{N}$)
x_v	molar flux of vapour per molar flux of two-phase mixture ($\dot{N}_v/\dot{N}$)
z	axial distance in the reactor (cm)

Greek symbols

β_v	volumetric flow rate fraction of vapour
κ	effective conductivity of the electrolyte (Ω^{-1} cm^{-1})
κ°	conductivity of bubble-free electrolyte (Ω^{-1} cm^{-1})
θ_v	volume fraction of vapour
ρ_{ave}	mass density of the two-phase mixture (g cm^{-3})
ρ'_{ave}	mass density of the two-phase mixture (g cm^{-3})
ρ_l	mass density of the liquid phase (g cm^{-3})
ρ_v	mass density of the vapour phase (g cm^{-3})
ρ_m	molar density of the two-phase mixture (mol cm^{-3})
$\rho_{m,l}$	molar density of the liquid phase (mol cm^{-3})
$\rho_{m,v}$	molar density of the vapour phase (mol cm^{-3})
σ	surface tension of the electrolyte (dyn cm^{-1} or N m^{-1})

1. Introduction

Recently, a forced convective, bipolar flow reactor [1] has been developed as a replacement to the Simons cell [2] for the electrochemical fluorination of organic compounds. Although this new design reduces energy costs and increases production rates, a better understanding of the process is needed to minimize operational problems and maximize production rates. To better understand the operation of the fluorination reactor, a series of models

have been developed [3–6]. These revealed that the fluorination reaction has operating characteristics not seen in other electrochemical reactors. For example, because the parasitic reaction (i.e., H_2 oxidation) involves a gaseous product, and the system operates at relatively high temperatures, the current efficiency in the fluorochemical reactor increases with cell current [4, 5]. Higher currents result in higher temperature, which increases evaporation of the HF and lowers the partial pressure of H_2. This is in contrast to recent models of more typical systems where the rate of the parasitic reaction (i.e., H_2 evolution) increases with current [7–9].

The two-phase flow resulting from the evolution of H_2 and the subsequent evaporation of HF also effects the current–voltage relationship of the reactor. The gas-phase reduces the effective conductivity of the electrolyte and increases the energy requirements of the system. Drake et al. [3] developed a steady-state model of the cell pack, and they studied cells with a 3.2 mm gap between the anode and cathode. At high operating voltages, where large amounts of gas are generated in the reactor, a transition in the two-phase flow from bubble to slug flow was predicted to occur inside the reactor. Considerably more slip occurs between the gas and the liquid during slug flow, which gives rise to an increase in the liquid-volume fraction at the transition point. The increased amount of liquid increases the effective conductivity of the electrolyte, which in turn increases the local current density (i.e., the local production rate of the fluorinated hydrocarbon).

We [4, 5] developed a similar steady-state model to that of Drake et al. [3], but we included interactions between the cell pack and the other sections of the fluorination reactor (e.g., inlet and outlet flow distributors). Our model also included the hydrogen oxidation reaction, which enabled us to predict current efficiency as a function of operating conditions. Experimental data from a bipolar flow reactor was used in conjunction with the model to extract the requisite kinetic parameter and mass-transfer coefficient [4]. Slip between the gas and liquid phases was neglected since the cells of interest had a thin anode to cathode gap (i.e., 0.8 mm), and the experimental results were at relatively high flow rates and low currents, where the vapour volume fractions were below 0.6.

Although the thin anode to cathode gap prevents slug flow from developing in the cell, operation at high currents and low flows where the vapour volume fractions exceeds 0.6 may violate the no-slip assumption. Therefore, in our subsequent dynamic model [6], we relaxed the no-slip assumption. However, no comparisons were made between simulated results where slip was and was not neglected. In this work, we present the effect of slip on the steady-state temperature, pressure, gas fraction, and current distribution in the reactor under relatively severe operating conditions. In addition, the effect of slip on the cell voltage, current efficiency and energy usage is shown at different flow rates over a wide current range.

2. Model development

2.1. *Description of the fluorination reactor*

The fluorination reactor (see Figure 1) is comprised of five sections: (1) inlet pipe, (2) inlet flow-distributors, (3) cell pack, (4) outlet flow-distributors, and (5) outlet pipe. The cell pack consists of 26 identical parallel-plate cells and each cell has 18 inlet and outlet flow distributors. The flow distributors are narrow channels evenly placed along the width of each cell, providing uniform flow to all the cells in the cell pack under normal operation.

Hydrogen evolution occurs at the cathode, and the following two reactions occur at the anode:

$$RH + 2F^- \rightarrow RF + HF + 2e^- \quad (A)$$

$$H_2 \rightarrow 2H^+ + 2e^- \quad (B)$$

where RF is the fluorinated organic compound, HF is anhydrous liquid hydrogen fluoride and RH is the fluorinatable organic compound. Complex nickel fluorides present in a thin anodic film catalyse the electrochemical fluorination reaction at the anode. Due to the use of an undivided cell, some of the hydrogen produced at the cathode is transported to, and oxidized at the anode. Therefore, the current efficiency of the electrochemical fluorination is less than unity. The overall reaction for the fluorination process can be represented as:

$$RH + HF \rightarrow RF + H_2 \quad (C)$$

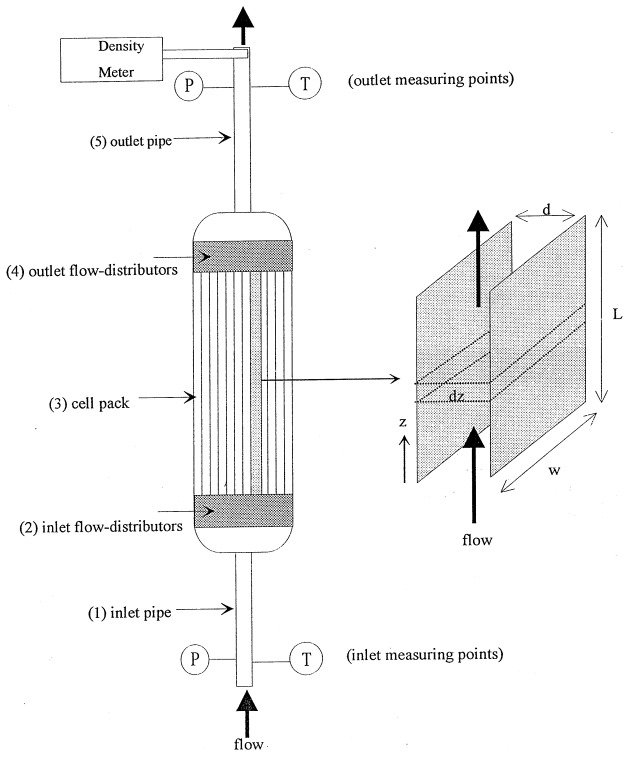

Fig. 1. Schematic of the electrochemical fluorination reactor. Inlet and outlet measurement points for temperature, pressure and density are indicated. A magnified view of one of the parallel-plate cells is also shown.

2.2. *Governing equations*

The assumptions used to model the electrochemical fluorination process are identical to those used in the previous work [5] except for the relaxation of the no-slip criteria. In other words, the vapour and liquid velocities are not necessarily equal. Therefore, only the governing equations that are affected by slip are shown here. The solution procedure used to solve the governing equations are also identical to that described previously [5].

As described previously [5], the electrical work done on the fluid in each cell depends on the effective conductivity of the electrolyte. The effective conductivity of the electrolyte is related to the pure electrolyte conductivity, κ°, and the volume fraction of the vapour phase, θ_v, by the Bruggeman equation as follows [10]:

$$\kappa = \kappa^{\circ}(1-\theta_v)^{1.5} \tag{1}$$

Equation 1 accounts for the shielding of the electrode by bubbles (i.e., bubble-curtain effect) by assuming that the bubbles are uniformly dispersed throughout the electrode gap. More recent studies have shown that in real systems the bubbles may be more randomly dispersed and chaotic [11]. The net effect is that Equation 1 may underpredict the effective conductivity of the electrolyte (i.e., overpredict the voltage loss due to bubble formation). The consequence of using Equation 1 will be discussed further in relation to the model results.

The volume fraction of vapour, θ_v, in Equation 1 is the volume occupied by the vapour per unit volume at each position in the reactor. Previously [5] it was assumed that there is no slip between the vapour and liquid phases. Therefore, the volume fraction of vapour, θ_v, was identical to the volumetric flow fraction of vapour, β_v, which is the ratio of the volumetric flow rate of the vapour to the volumetric flow rate of the two-phase mixture. However, for the case of slip between the vapour and liquid phases, θ_v is lower than β_v, as the velocity of the vapour is more than that of the liquid phase. For narrow channels having a separation distance of 0.8–3.0 mm, the buoyancy effects can be neglected and θ_v can be related to β_v by the following equation [12]:

$$\theta_v = 0.8\,\beta_v \tag{2}$$

The above correlation, obtained for an air-water system, is used due to a lack of experimental data regarding slip for the hydrogen–HF system. Although the density of the two systems are comparable, it is expected that the lower surface tension of HF compared to water ($\sim 6\times10^{-3}$ N m^{-1} for HF and $\sim 70\times10^{-3}$ N m^{-1} for water) will result in less slipping of the vapour past the liquid [13]. Therefore, the results shown here should be considered an upper bound to the degree of slip occurring between the vapour and liquid for the hydrogen–HF system. It is reasonable to expect though that the use of Equation 2 is closer to reality than to assume no slip (i.e., $\theta_v = \beta_v$).

The volumetric flow fraction, β_v, is related to the molar flow fraction of the vapour, the partial molar density of the vapour, and the average molar density of the two-phase mixture by the following equation:

$$\beta_v = \frac{x_v \rho_m}{\rho_{m,v}} \tag{3}$$

Equations 2 and 3 are used to calculate the volume fraction of vapour in the cells of the cell pack and the inlet and outlet flow distributors. However, Equation 2 should not used for the outlet pipe as it has a diameter much greater than 3 mm. The distribution parameter theory [13–15] is used to calculate the volume fraction of vapour in the outlet pipe by the following equation:

$$\theta_v = \frac{v_v}{1.1v + v_{v,drift}} \tag{4}$$

where v_v is the superficial vapour velocity, v is the two-phase mixture velocity, and $v_{v,drift}$ is the drift velocity of the vapour. The vapour velocity is calculated as

$$v_v = \frac{\dot{N} x_v}{\rho_{m,v}} \tag{5}$$

The two-phase mixture velocity is the sum of the superficial velocities of the liquid and vapour phases and expressed as

$$v = \frac{\dot{N} x_v}{\rho_{m,v}} + \frac{\dot{N} x_l}{\rho_{m,l}} \tag{6}$$

In general, the vapour drift velocity, $v_{v,drift}$, used in Equation 4, is related to the two-phase flow regime and orientation, size of the vapour bubbles and the electrolyte surface tension, density and viscosity [13]. Although the bubble sizes are difficult to measure or predict, the turbulent flow present in the outlet pipe enables one to obtain a reasonable estimate of the drift velocity without knowledge of the bubble size [13, 15]:

$$v_{v,drift} = 3.28\left(\frac{\sigma g}{\rho_l}\right)^{0.25} \tag{7}$$

The surface tension of HF used in the simulations is 6 dyne cm^{-1} (i.e., 6×10^{-3} N m^{-1}).

The pressure drop is composed of contributions from the elevation, frictional, and kinetic pressure drops. The equations for these pressure drops are the same as given previously [5], but some of the terms in these equations are different due to the removal of the no-slip assumption. For one, the velocity used in the calculations for the kinetic and frictional pressure drops is the mixture velocity, v, given by Equation 6. Also, in calculating the kinetic pressure drop, the two-phase density based on

the volumetric flow rate fractions, ρ'_{ave}, should be used instead of that based on the volume fractions of the vapour and liquid phases, ρ_{ave}. (see [5] for ρ_{ave} relationship). This is because the energy entering and leaving a differential element of the flow section is a function of the properties of the fluid entering and leaving the differential element, not of the fluid in the volume element [17]. The two-phase density, ρ'_{ave}, can be expressed as a function of the volumetric flow rate fraction of vapour, β_v, and the densities of the vapour and liquid phases by the following equation:

$$\rho'_{ave} = (1 - \beta_v)\rho_l + \beta_v\rho_v \tag{8}$$

When there is slip between the vapour and liquid, the friction factor multiplier, f', is calculated by the following equation obtained by fitting the predictions of Beggs and Brill [17] over the vapour volume fraction range of 0–1:

$$f' = 1.234 + 0.315 \ln\left(\frac{1 - \beta_v}{(1 - \theta_v)^2}\right) \tag{9}$$

Note that the above equation reduces to Equation 43 in the previous work [5] when the no-slip criteria is used (i.e., the volume fraction of vapour, θ_v is equal to volumetric flow fraction of vapour, β_v).

3. Results and discussion

The effect of slip on the distribution of the dependent variables in the reactor (i.e., temperature, pressure, gas fraction and current) is presented for selected cases where the operating conditions are relatively severe. Conversely, the effect of slip on the cell voltage, current efficiency and energy usage is shown at different flow rates over a wide current range, where the conditions vary from mild to severe. Unless otherwise noted, the values for the cell dimensions, physical parameters, and operating conditions are either listed in Table 1, or given in reference [5]. The choice of independent variables (i.e., inlet temperature and flow rate, current and outlet pressure) is consistent with the operation of an actual fluorination reactor [4].

3.1. *Profiles of dependent variables in the reactor*

Figure 2 shows the pressure profiles in the fluorination reactor when slip between the gas and the liquid is either neglected or included in the model. Note that the outlet pressure is controlled at the specified value (i.e., 2.0 atm) and the pressures throughout the reactor are calculated. These profiles indicate that the pressure drops are steep ($\sim$1.5 atm m^{-1}) in the outlet flow distributors (i.e., section 4), and gradual in the rest of the fluorination reactor sections. Further, entrance and exit effects are present in the outlet flow distributor, which produce a steep pressure drop as the fluid enters the flow distributor and a correspondingly steep pressure rise as it exits. Entrance and exit effects are negligible in other reactor sections. The higher pressure gradients in the outlet flow distributors are due to frictional effects resulting from higher flow velocities. The higher velocities arise from the lower cross sectional area available for the two-phase fluid flow. The pressure gradients in the outlet flow distributor are more pronounced than at the inlet because of the higher vapour volume fraction and hence higher two-phase velocity. The pressure drops in all the sections except the flow distributors are mainly composed of the elevation pressure drop because fluid velocities in these sections are low.

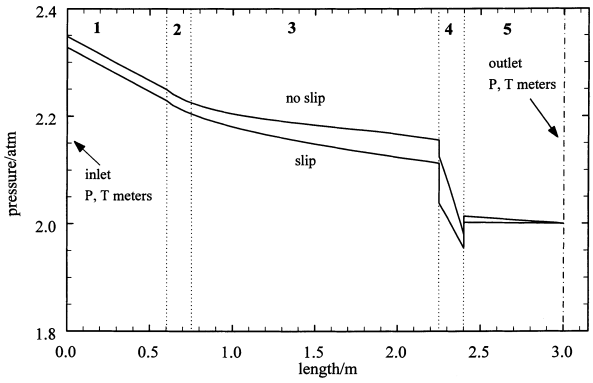

Fig. 2. Pressure profiles in the fluorination reactor when slip between the gas and liquid phase is either neglected or included in the model. Numbered sections: (1) inlet pipe, (2) inlet flow distributor, (3) cell pack, (4) outlet flow distributor and (5) outlet pipe. Operating conditions are given in Table 1.

Table 1. Operating conditions used in obtaining simulation results presented in Figures 2–8, unless otherwise stated

Inlet temperature	32 °C
Inlet flow rate	1.8 l s^{-1}
Current	700 A
Outlet pressure	2.0 atm

The pressure drop in the outlet flow distributors is higher in the case of no-slip compared to slip due to a higher two-phase velocity. The higher velocity results in higher frictional and kinetic pressure drops. The two-phase velocity is higher in the case of no-slip because the liquid is constrained to move at the same velocity as the gas. Since the liquid density is considerable larger than that of the gas, this density-averaged velocity (see Equation 6) is greater. In the case of slip, the low-density gas moves at a higher velocity than the liquid, resulting in a lower two-phase velocity. Conversely, the pressure drop in the cell pack is lower for the case no-slip due to higher vapour volume fractions, and therefore lower fluid density. The lower fluid density results in a lower elevation pressure drop, which is the dominant component of the pressure drop in the cell pack.

Figure 3 shows the temperature profiles in the fluorination reactor when slip between the gas and the liquid is either neglected or included in the model. Note that the

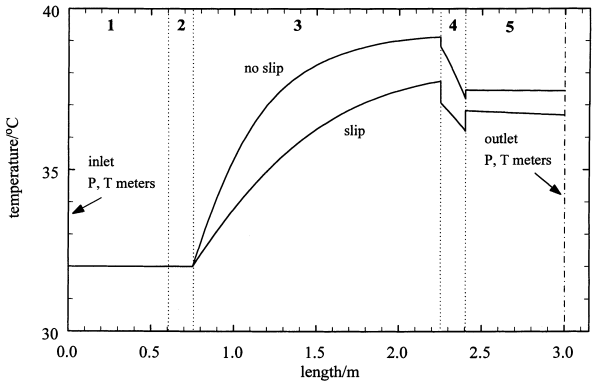

Fig. 3. Temperature profiles in the fluorination reactor when slip between the gas and liquid phase is either neglected or included in the model. Numbered sections: (1) inlet pipe, (2) inlet flow distributor, (3) cell pack, (4) outlet flow distributor and (5) outlet pipe. Operating conditions are given in Table 1.

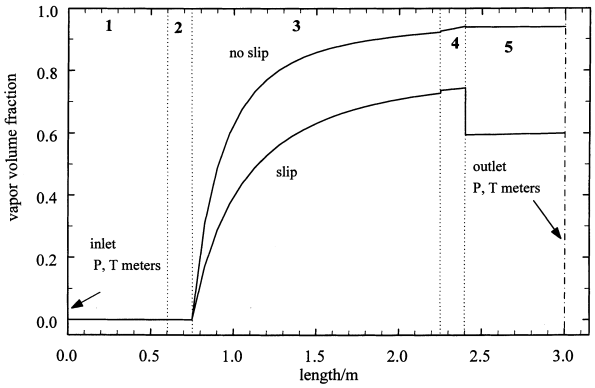

Fig. 4. Volume-fraction profiles in the fluorination reactor when slip between the gas and liquid phase is either neglected or included in the model. Numbered sections: (1) inlet pipe, (2) inlet flow distributor, (3) cell pack, (4) outlet flow distributor and (5) outlet pipe. Operating conditions are given in Table 1.

inlet temperature is controlled at the specified value (i.e., 32 °C) and the temperatures throughout the reactor are calculated. These profiles indicate that the temperatures are constant in the inlet pipe and the inlet flow distributors, rise in the cell pack, drop in the outlet flow distributors and decrease marginally in the outlet pipe. There is no temperature change in the first two flow sections since there is no energy input and the fluid is all liquid. The temperature increases along the length of the cell pack due to the electrochemical power input. However, the temperature decreases in the outlet flow distributors due to a decrease in pressure leading to the adiabatic evaporation of liquid HF. There is a marginal temperature decrease in the outlet pipe also due to adiabatic vaporization. The maximum temperature in the fluorination reactor occurs in the cell pack, which in Figure 3 is about 2 °C greater than the outlet temperature. The temperatures in the flow cell are higher in the case of no-slip due to higher vapour volume fractions. The higher vapour volume fractions lead to lower effective electrolyte conductivities, and hence higher ohmic heating.

The changes in pressure and temperature affect the vapour volume fractions in each of the fluorination reactor sections as shown in Figure 4. There is no vapour fraction in the inlet pipe and flow distributors due to a single-phase (liquid) feed and no vapour generation in these sections. The vapour volume fraction increases throughout the cell pack due to the accumulation of hydrogen gas produced in the cell pack and the subsequent HF evaporation. The amount of gas in the reactor is a strong function of the cell current and fluorochemical production efficiency. The volume of vapour is, however, also dependent on the local pressure and temperature. For the case shown in Figures 2–4 though, the effect of temperature and pressure on the vapour volume fraction in the outlet flow distributor cancel each other out. The pressure drop seen in Figure 2 would tend to increase the evaporation of HF and the temperature decrease seen in Figure 3 would tend to decrease HF evaporation. The result is that the vapour volume fraction is relatively unchanged in the outlet flow distributor even though the change in temperature and pressure is dramatic.

Figure 5 shows the current density throughout the cell pack for the case of slip and no-slip. The higher vapour volume fractions predicted for the case of no-slip (see Figure 4) result in lower effective electrolyte conductivities. The lower conductivities at the cell-pack outlet force the current towards the entrance to the cell pack. The effect of bubbles on the current distribution is not very significant when θ_v is less than 0.8. Such a condition exists when slip of the vapour past the liquid is allowed (i.e., according to Equation 2, θ_v can not exceed 0.8). Therefore, even though the vapour volume fraction shown in Figure 4 for the case of slip changes significantly from inlet to outlet, the resulting current distribution shown in Figure 5 is relatively uniform. A relatively uniform reaction was predicted even though Equation 1 is expected to underpredict the effective conductivity of the electrolyte [11]. A key conclusion that can be drawn from Figure 5 is that the self-

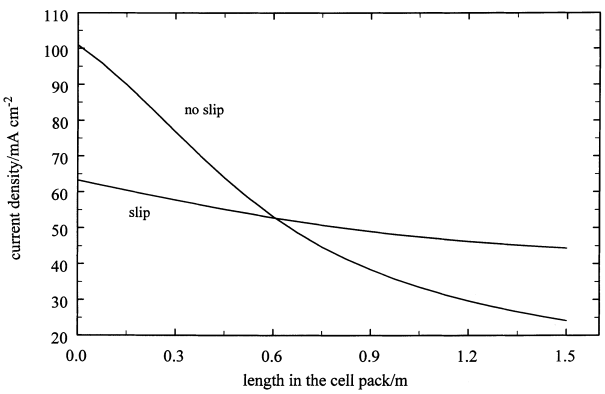

Fig. 5. Current distribution in the cell pack when slip between the gas and liquid phase is either neglected or included in the model. Operating conditions are given in Table 1.

regulating nature of the flow reactor should result in relatively uniform current distributions under most realistic operating conditions. This conclusion should hold even if the use of Equation 2 overpredicts the extent of slip between the vapour and liquid.

3.2. *Effect of operating conditions on the cell pack voltage and current efficiency*

The effect of slip between the vapour and liquid phases on the steady-state behaviour of the reactor is shown in Figures 6–8. In each Figure, the filled and open symbols are results from discrete simulations for the cases with and without slip, respectively, and the lines are used to join the simulation points. The results for the case of no-slip have already been presented in the earlier paper [5] but are replotted here for comparison with the case of slip. Under the normal operating conditions studied previously [5] (i.e., inlet flow rate $>3.0\ \mathrm{l\ s^{-1}}$ and applied current <500 A), the no-slip assumption is valid since the dashed and solid lines are converging in this region. However, extension of the model results to more extreme operating conditions requires a relaxation of this assumption.

Figure 6 shows that slip between vapour and liquid phases has a large effect on the prediction of the cell voltage. The steep rise in cell voltage seen for the case of no-slip is due to an exponential increase in the ohmic contribution to the cell voltage at values of vapour volume fraction greater than 0.9. However, when the no-slip condition is relaxed, this situation does not occur because the extent of slip between the vapour and liquid increases as the vapour volume fraction increases. For narrow channels having a separation distance of 0.8–3.0 mm, which covers the separations in the reactor studied here, $\theta_v \leq 0.8$ (see Equation 2). The reactor becomes self-regulating, and increasing the amount of vapour increases its velocity but not necessarily its volume fraction. As pointed out during the discussion of Figure 5, the self-regulating nature of the flow reactor should occur even if the use of Equation 2 overpredicts the extent of slip between the vapour and liquid.

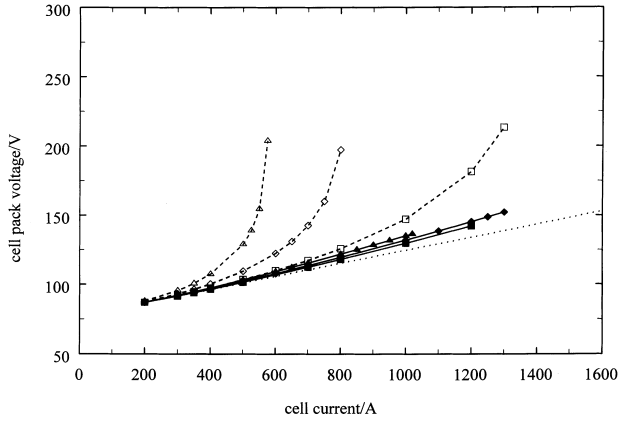

Fig. 6. Cell pack voltage predicted by the model for cases of slip (filled symbols; solid line) and no slip (open symbols; dashed line) for various cell currents and electrolyte feed flow rates. Symbols represent discrete simulations, and lines connect those symbols. Results represented by the three different filled symbols are visually indistinguishable from each other. Key: (▲, △) $1.2\ \mathrm{l\ s^{-1}}$; (◆, ◇) $1.8\ \mathrm{l\ s^{-1}}$; (■, □) $3.0\ \mathrm{l\ s^{-1}}$.

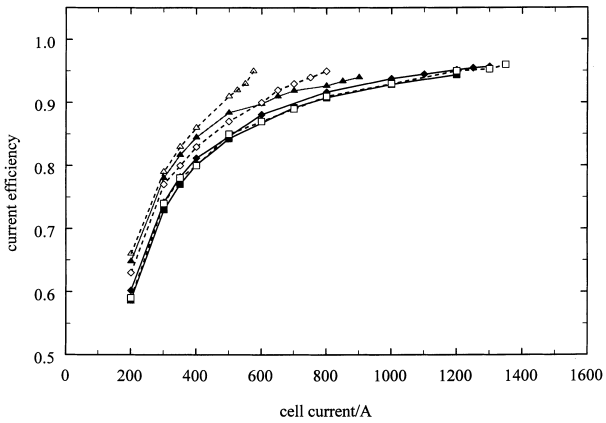

Fig. 7. Current efficiency predicted by the model for cases of slip (filled symbols; solid line) and no slip (open symbols; dashed line) for various cell currents and electrolyte feed flow rates. Symbols represent discrete simulations, and lines connect those symbols. Key: (▲, △) $1.2\ \mathrm{l\ s^{-1}}$; (◆, ◇) $1.8\ \mathrm{l\ s^{-1}}$; (■, □) $3.0\ \mathrm{l\ s^{-1}}$.

For the simulation results in Figure 6, the deviation of the cell voltage from open circuit is due mainly to ohmic resistance. The dotted line in Figure 6 is for the limiting case where the bubbles do not influence the electrolyte conductivity. The slope of this line is approximately $(nd/wL\kappa^{\circ})$, which indicates ohmic resistance dominates. The proximity of the solid symbols to the dotted line indicates that the bubbles have a small effect on the ohmic losses in the cell. Therefore, even though Equation 1 overpredicts the voltage loss due to bubble formation, its use compared to other correlations will have a small effect on the voltage predictions with slip. The no-slip predictions on the other hand are greatly affected by bubble formation. Therefore, the use of Equation 1 means that the open symbols in Figure 6 are an upper voltage limit for this system. The significant

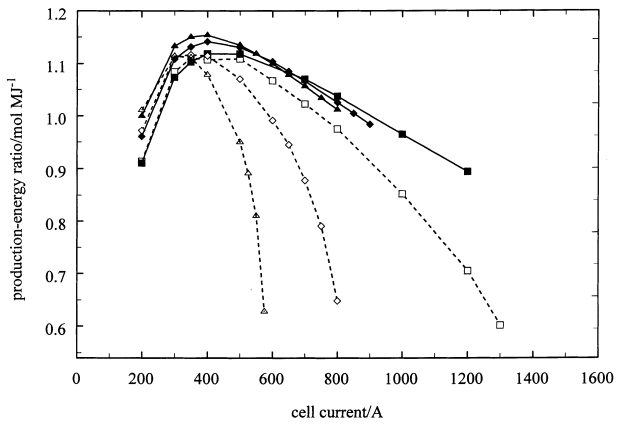

Fig. 8. Production/energy ratio predicted by the model for cases of slip (filled symbols; solid line) and no slip (open symbols; dashed line) for various cell currents and electrolyte feed flow rates. Symbols represent discrete simulations, and lines connect those symbols. Key: (▲, △) $1.2\ \mathrm{l\ s^{-1}}$; (◆, ◇) $1.8\ \mathrm{l\ s^{-1}}$; (■, □) $3.0\ \mathrm{l\ s^{-1}}$.

difference between the solid and dashed lines in Figure 6 also emphasizes the sensitivity of the cell voltage to the extent of slip occurring in the reactor.

The current efficiencies, as shown in Figure 7, are not greatly affected by slip of the vapour past the liquid. However, the efficiencies with slip do plateau at lower values of cell current compared to cases without slip. In both cases, the efficiency increases with cell current. Higher cell currents lead to greater cell temperatures and therefore, more evaporation of HF. The higher HF concentration in the vapour phase leads to lower hydrogen partial pressures and consequently lower hydrogen reoxidation current. A lower hydrogen reoxidation current coupled to a higher applied cell current results in a significant drop in the *fraction* of current going into hydrogen oxidation (i.e., higher efficiencies). The efficiencies would asymptote to unity at infinite cell current.

The results in Figures 6 and 7 can be combined to give Figure 8. The ordinate in Figure 8, labelled production/energy ratio, is obtained by dividing the fluorochemical production rate (proportional to efficiency $\times$ current) by the power input (current $\times$ cell voltage). The production/energy ratio shows a maximum at about the same values of the cell current for the cases of slip as well as no-slip. The two sets of curves deviate at currents beyond this maximum due to an extreme overprediction of cell voltage at high currents for the case of no slip. However, for normal operating conditions (i.e., inlet flow rate $>3.0\,\mathrm{l\,s^{-1}}$ and applied current <500 A), the difference in the values of the production/energy ratio for cases of slip and no slip is minimal.

Though the vapour volume fraction predicted for the case of slip between the vapour and liquid does not reach the levels obtained for the case of no-slip, it should be remembered that the correlations used in this work for predicting the vapour fraction are extracted for the air–water system. The lower surface tension of HF compared to water would lead to smaller bubbles [13], resulting in more bubbly flow and hence less slip. Therefore, the correlation used here may underpredict the vapour fractions present in the hydrogen–HF system. The actual values for the vapour volume fraction would be intermediate of those obtained for the cases of slip and no-slip between the vapour and liquid phases, but probably closer to the case of slip.

Although the equation used to predict slip may underestimate the vapour volume fraction, the effective conductivity predicted from Equation 1 may overestimate the effect of bubbles on the voltage losses in the cell [11]. These two assumptions, therefore, offset each other and bring the voltage predictions with slip closer to reality. The extent to which they offset each other, however, can not be determined.

Finally, based on the comparison of model simulations to experimental data at low currents, it is assumed that the kinetic parameter and mass-transfer coefficient are not a function of operating conditions [4]. This assumption is justified by the fact that at low currents slip is negligible, and at high currents the voltage is ohmically limited and the hydrogen oxidation current is negligible (i.e., the current efficiency approaches 1.0).

4. Conclusion

A mathematical model was used to study the effect of slip between the gas and liquid phases on the performance of an electrochemical fluorination reactor. The model incorporates two-phase flow with differential material, energy and pressure balances. The effect of slip on the cell voltage, and hence energy usage, is insignificant under normal operating conditions, but it is significant at high cell currents and low flow rates. Slip of the vapour past the liquid lowers the amount of vapour in the reactor, which in turn increases the effective conductivity of the electrolyte and lowers the cell voltage. The reactor actually becomes self-regulating since increasing the current or decreasing the flow rate increases the gas-phase velocity relative to the liquid.

The ability to accurately predict the extent of this self-regulation, however, is very sensitive to the correlation used to predict the vapour volume fraction. The correlation used here may underpredict the vapour fractions present in the hydrogen–HF system. The actual vapour volume fractions would be intermediate of those obtained for the cases of slip and no-slip between the vapour and liquid phases, but probably closer to the case of slip. Conversely, the correlation used to relate the effective conductivity to the vapour fraction may overestimate the effect of bubbles on the voltage losses in the cell. The net effect of underestimating the vapour fraction and overestimating the electrolyte resistance should bring the voltage predictions with slip closer to reality. The extent to which they offset each other, however, can not be determined.

Acknowledgement

This work was made possible by financial support from 3M Company.

References

1. W.V. Childs, F.W. Klink, J.C. Smeltzer and J.C. Spangler, *US patent 5 322 597* (21 June 1994).
2. J.H. Simons, *in* J. Simons (Ed.), 'Fluorine Chemistry' (Academic Press, New York, 1950), p. 414.
3. J.A. Drake, J. Newman and C.J. Radke, *J. Electrochem. Soc.* **145** (1998) 1578.
4. K. Jha, PhD. thesis, University of South Carolina, Columbia, SC (1998).
5. K. Jha, G.L. Bauer and J.W. Weidner, *J. Electrochem. Soc.* **145** (1998) 3521.
6. K. Jha, G.L. Bauer and J.W. Weidner, *J. Appl. Electrochem.* **30** (2000) 85–93.
7. S. Prasad, J.W. Weidner and A.E. Farell, *J. Electrochem. Soc.* **142** (1995) 3815.

8. D. Coleman, R.E. White and D.T. Hobbs, *J. Electrochem. Soc.* **142** (1995) 1152.
9. M.M. Saleh, J.W. Weidner, B.E. El-Anadouli and B.G. Ateya, *J. Electrochem. Soc.* **144** (1997) 922.
10. D. Bruggeman, *Ann. Physik*. **24** (1935) 636.
11. S. Kisdnasamy and P.S. Neelakantaswamy, *J. Appl. Electrochem.* **14** (1984) 749.
12. M. Ali, M. Sadatomi and M. Kawaji, *Canadian J. Chem. Eng.* **71** (1993) 657.
13. G. Wallis, 'One-Dimensional Two-Phase Flow' (McGraw-Hill, New York, 1969).
14. R. Dowlati, M. Kawaji, D. Chisholm and A.M. Chan, *AIChE J.* **38** (1992) 619.
15. N. Clark and R. Flemmer, *AIChE J.* **31** (1985) 500.
16. D. Kern, 'Process Heat Transfer Engineers' Handbook' (International Ed., McGraw-Hill, New York, 1965).
17. H. Beggs and J. Brill, *J. Petroleum Tech.* (May 1973) 607.